THE LEONID METEOROID STREAM: SPACECRAFT INTERACTIONS AND EFFECTS

J.A.M. McDonnell, N. McBride, D.J. Gardner

Unit for Space Sciences and Astrophysics
The Physics Laboratory, The University of Kent, Canterbury, CT2 7NR, UK
Tel +44 (0)1227 459616, Fax +44 (0)1227 762616, Email J.A.M.McDonnell@ukc.ac.uk

ABSTRACT

The Leonid meteor shower is characterised by an intense, albeit irregular, flux rate. Forthcoming showers from 1997 to 2000 have the potential to exceed the sporadic meteoroid background by several orders of magnitude at peak, and high velocities can lead to very high efficiency of charge generation. This paper considers effects such as penetration damage to satellites in LEO and GEO. Impact velocities are considered, and formulae for penetration and plasma charge and current production are presented. It is found that the Leonids exceed any other stream in terms of plasma current generation even under normal 'quiescent' conditions. During the storm flux enhancement, several catastrophic events might be expected in the satellite population.

1. INTRODUCTION

The possibility of meteoroid-related loss of a satellite has been examined in relation to the Olympus communications satellite and the Perseid meteor shower (Caswell *et al.* 1995). In next few years, the Leonid meteor shower offers the potential of considerable risk to the satellite population (Beech & Brown 1994; Beech *et al.* 1995). In this paper we consider specifically, the impact effects that will be encountered during the Leonid activity.

Meteor detection rates for previous apparitions of the Leonid shower are given by Jenniskens (1995; see Fig. 2 in that paper) for 1866, 1867, 1966 and 1969. Essential to the prediction of potential damage effects in space is the peak height (zenithal hourly rate, ZHR) and its width. An exceptionally high peak rate of 150,000 (ZHR) was observed in 1966 (compared to normal activity of around 25 ZHR), although Jenniskens notes this rate may be in error, and the actual rate might have been around 15,000 (ZHR). The width of the 'storm' activity was less than 0.1° of solar longitude which translates to < 2.4 hours on Earth. Thus only for specific longitudes will the storm activity be visible in the 4 years considered (1997 to 2000). For GEO satellites, the danger will be predictable in terms of preferred impact directions.

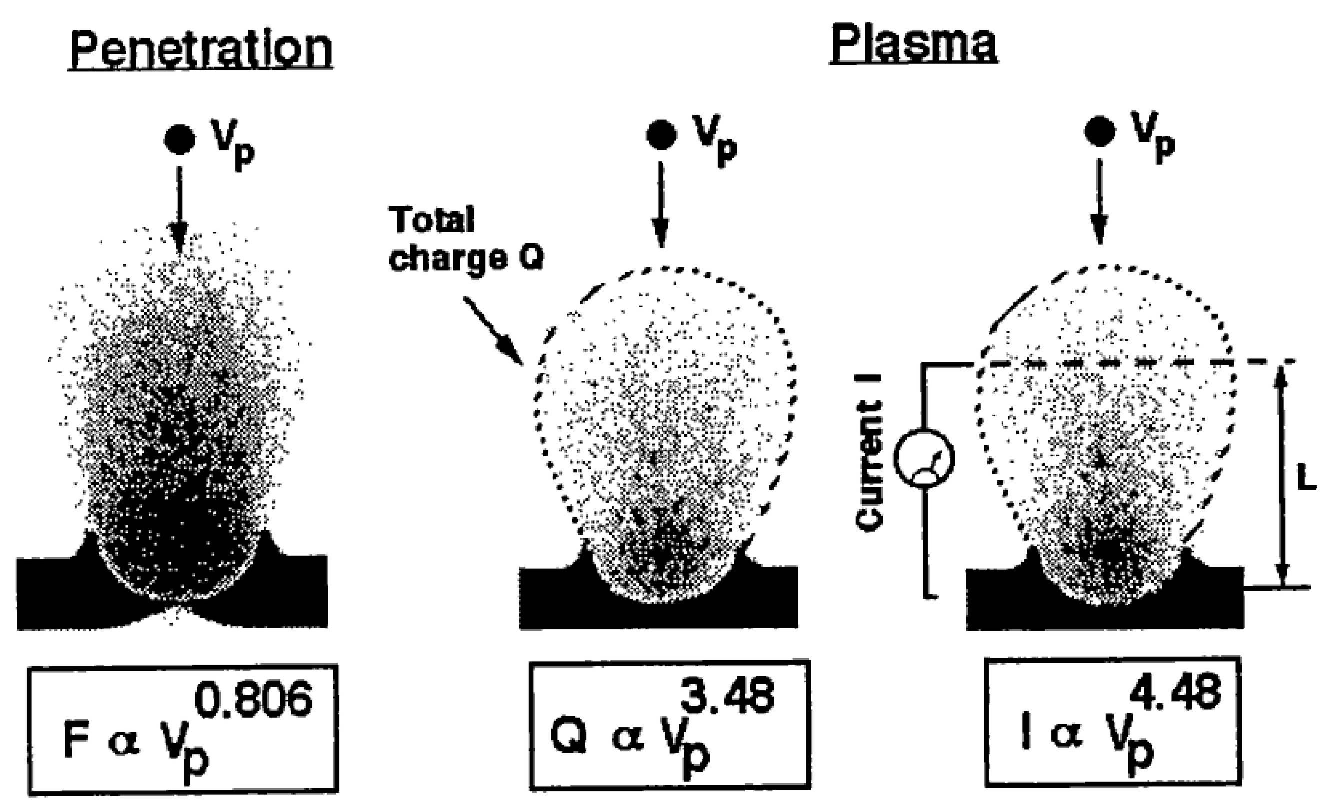

Figure 1: A comparison the impact effects when considering penetration (F), charge production (Q) and plasma current (I).

2. IMPACT EFFECTS

Although light gas guns have limited velocity range and certainly do not extend to the Leonid impact speed of some 71 km s^{-1}, we have, using other techniques, studied penetration to 16 km s^{-1} (Gardner *et al.* 1997) and impact plasma to > 100 km s^{-1} using the University of Kent's 2 MV dust accelerator. In light of this it is sufficient, for a first prediction of likely effects, to use velocity scaling to extrapolate to the required impact velocity relevant for the Leonids. We use the penetration formula given by McDonnell & Sullivan (1992) based on penetration studies up to

Proceedings of the Second European Conference on Space Debris, ESOC, Darmstadt, Germany, 17-19 March 1997, (ESA SP-393, May 1997)

16 km s^{-1}:

$$\frac{F_{max}}{d_p} = 1.272 d_p^{0.056} V^{0.806} \times \left(\frac{\rho_p \rho_{\rm Al}}{\rho_{\rm Fe} \rho_t}\right)^{0.476} \left(\frac{\sigma_{\rm Al}}{\sigma_t}\right)^{0.134} , \quad (1)$$

where particle diameter d_p and F_{max} are in cm, and velocity V is in km s^{-1}. A velocity exponent of 0.806 applies and only a weak dimensional scaling of $d_p^{1.056}$. For plasma charge production, which is exploited on real-time detectors such as the Ulysses and Galileo missions in deep space, the charge produced generally follows a relationship proportional to $\sim mV^{3.5}$ (Dietzel *et al.* 1973). However incorporating further calibration from accelerator tests, we use the explicit relationship:

$$Q = 0.1m \left(\frac{m}{10^{-11}}\right)^{0.02} \left(\frac{V_p}{5}\right)^{3.48} , \quad (2)$$

where Q is in coulombs, mass m is in g and particle velocity V_p is in km s^{-1}. This charge is detected under the application of a small electric field (~ 5 V cm^{-1}) and leads to approximately equal positive and negative charges on the relevant electrodes. In the absence of an applied field a charge is still generated due to the differing velocity of the electron and ion components although the main velocity involved is that of the bulk plasma/ejecta expulsion velocity. On a spacecraft pre-existing surface charges from exposed dielectrics can provide adequate electric fields although the resistivity will readily limit the current which can be drawn from the plasma. Certainly the plasma can neutralise such surface charges in a time of order microseconds. However, where we do have exposed conductors such as solar array bus structures or unprotected umbilicals the current pulse may be high. Since the current pulse is given by the rate of change of charge arriving at a conductor and the arrival velocity is related to the ejecta velocity, the velocity exponent is effectively increased by 1, in the current dependence. The characteristic time over which Q is measured is $\sim L/V_p$ where L is the plasma path length and hence a functional form for this current I (which is $\partial Q/\partial t$) is

$$I = 0.1m \left(\frac{m}{10^{-11}}\right)^{0.02} \left(\frac{V_p}{5}\right)^{3.48} \frac{V_p}{L} , \quad (3)$$

where m is in g, L is in km, V_p is in km s^{-1}, and I is in A.

For momentum transferred to the target we have a weaker velocity dependence. The momentum enhancement, ϵ, relative to the incident particle has been measured during calibration of the Giotto shield sensor of DIDSY. This gives an empirical relation (see McDonnell *et al.* 1984)

$$\epsilon = 1 + 0.3(V_p - 2) , \quad (4)$$

where V_p is in km s^{-1}. We can use these functional relationships to establish appropriately weighted velocities and their effect on spacecraft for both the sporadic meteoroids, space debris or a meteoroid stream such as the Leonids. Appropriate parameters for selected typical orbits are now presented.

3. ENCOUNTER VELOCITIES

Using a geocentric encounter velocity for the Leonid meteoroid stream of $V = 71$ km s^{-1} (at the top of the atmosphere), we can consider the typical impact velocity to a LEO spacecraft, with inclination 28.5° at an altitude $h = 500$ km (in a circular orbit). We find a mean impact velocity of ~71.2 km s^{-1}. The maximum and minimum impact velocity, as the spacecraft orbits, gives a variation of ±7.6 km s^{-1}. For a geostationary orbit the corresponding velocity is 70.3 ± 3.1 km s^{-1}, and for a LEO polar orbit of 500 km, the value is 71.4 ± 7.6 km s^{-1}. In the ~10μm–mm impactor size range the distribution is dominated by meteoroids, the global mass distribution of which is well described by Grün *et al.* (1985). The velocity applicable to this impactor range is derived from radar meteor data. We use the distribution from Taylor (1995a; 1995b) which is from a re-analysis (and correction) of the Harvard Radio Meteor Project data (Southworth & Sekanina 1973; Sekanina & Southworth 1975).

Spacecraft effect	Sporadics mean vel.	Leonids vel.	Leonids E factor
True mean (const. mass)	17.9	71	4.0
Penetration ($\gamma = 2.29$)	25.8	71	10.2
Plasma charge ($\gamma = 3.41$)	31.0	71	16.9
Plasma current ($\gamma = 4.39$)	36.1	71	19.5

Table 1: Velocity weighted means, appropriate to given detection techniques, and the mass threshold enhancement factor E of the Leonids over the sporadics (see text).

The velocity distribution is derived, in the first instance, at the top of the atmosphere (where the meteors are produced *i.e.* ~100 km altitude) but can be transformed to V_∞ or applied to arbitrary satellite positions and orbits (see McBride *et al.* 1996). The velocity distribution re-analysis now shows a higher proportion of faster meteoroids. For any observational technique the limiting threshold is a combination of factors and the derived mass distribution and fluxes reflect the method of acquisition. If a *mean* velocity is needed to represent the entire velocity distribution, then the mean should be calculated, weighted with the various factors relevant to the detection technique.

If the cumulative flux of particles over a given mass range can be described by $F(m) = km^{-\alpha}$, where α is the cumulative mass distribution index and k is a constant, then the ratio of fluxes for masses m_1 and m_2 is simply given by $F(m_2)/F(m_1)$ which is $(m_2/m_1)^{-\alpha}$. However a sensor detects parameters such as penetration limit, plasma production etc, which depend on mass and velocity such that

$$\text{signal} = c\ M^a\ V^b \tag{5}$$

where c is a constant. Hence the ratio of the number of detections for two particle velocities V_1 and V_2 will be given by

$$\frac{F(V_2)}{F(V_1)} = \left(\frac{V_2}{V_1}\right)^{(\alpha b/a)} \tag{6}$$

where the ratio b/a is often referred to as the factor γ. Thus in order to convert from an *equal mass* velocity distribution to an *equal detection threshold* velocity distribution one must weight the distribution by the factor $V^{\alpha\gamma}$. For example, it is seen from Eq. 1 that $F_{max} \propto d_p^{1.056}V^{0.806}$ *i.e.* $m^{0.352}V^{0.806}$, hence $\gamma = 0.806/0.352 = 2.29$. Table 1 gives the weighted mean velocities (calculated using $\alpha = 1.1$ which is applicable to the mass regime being considered) which can be used as a single velocity in the respective formulae for particular phenomena (Eqs. 1–4). The table also shows the 'enhancement factor' that occurs when considering the Leonid meteoroid stream. This can be thought of as the factor (in mass) by which the detection threshold shifts for a given detection threshold system. For example, the 'just detected' particles from the Leonids will be a factor 19.5 less massive than the typical sporadic component, and thus detections will be more numerous by the appropriate factor governed by the mass distribution index.

4. ENCOUNTER EPOCH AND GEOMETRY

Detailed analysis of the expected solar longitude of Leonid storm activity was performed by Beech *et al.* (1997), and was found to be 235.16 ± 0.04°. The epoch of the stream's arrival at the Earth is readily computed and the radiant established. Fig. 2 shows the geometry for 1999. The radiant is 2.8° sunwards of the Earth Apex of motion direction and inclined at +10° from the ecliptic. Also shown are the position of potentially favourable night time visibility from the Earth. Table 2 shows useful geometry information for potential storms for 1997, 1998, 1999 and 2000.

Year	Radiant from apex	Greenwich from apex	Longitude of visibility
1997	2.8°	72.5°	210°E–270°E
1998	2.8°	164.2°	125°E–185°E
1999	2.8°	255.6°	30°E–90°E
2000	2.8°	349.3°	295°E–355°E

Table 2: Useful geometry information for the 1997, 1998, 1999 and 2000 Leonids. Angles of radiant and Greenwich are measured from the Earth apex direction, towards the solar direction.

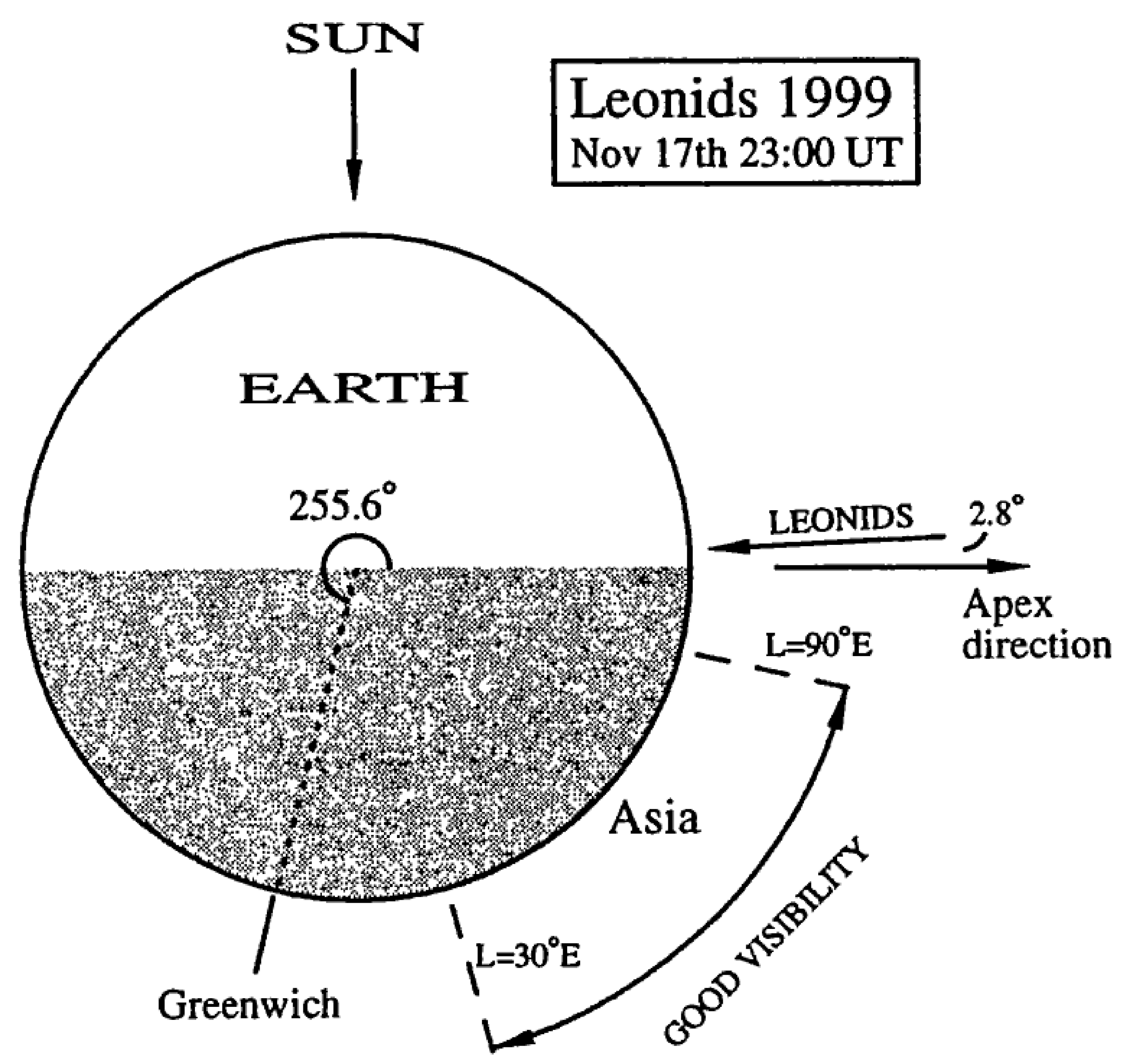

Figure 2: The geometry of the 1999 Leonid encounter at time of storm maximum. The region of good visibility is indicated. Note LEO satellites are generally shielded from the stream for half their orbit.

5. IMPACT PHENOMENA

Consider first the effect of impact penetration of a spacecraft surface. We can consider the role of the annual Leonids stream (*i.e.* not enhanced) by comparing the instantaneous flux at a given penetration limit from all the major meteoroid streams, and also from the sporadic dust environment in general.

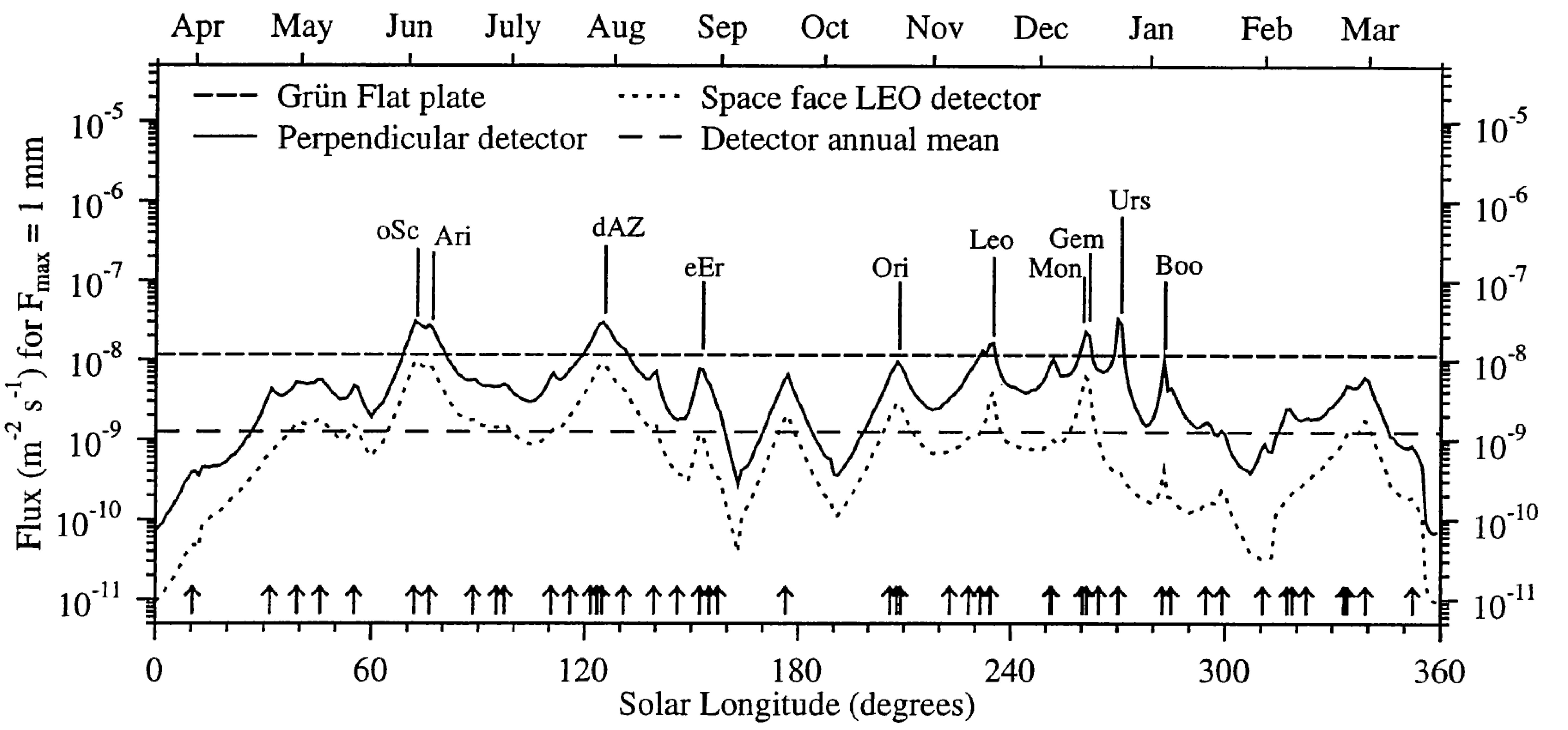

Figure 3: Instantaneous flux throughout the year, of stream meteoroids that penetrate 1 mm of aluminium foil (*i.e.* $F_{max} = 1$ mm). The arrows indicate the peaks of all 50 streams used (following Jenniskens 1994), with the 10 most important streams labelled: Ursids (Urs), δ Aquarids South (dAZ), ω Scorpiids (oSc), Geminids (Gem), daytime Arietids (Ari), Leonids (Leo), Bootids (Boo), Orionids (Ori), Monocerotids (Mon) and ϵ Eridanids (eEr).

McBride (1997) used the 50 most prominent annual meteoroid streams, as compiled by Jenniskens (1994). A consideration of meteor shower fluxes and stream speeds etc, led to a determination of the flux distribution of the streams. For the Leonids (not enhanced), the flux distribution was given by a relation $F(\mathrm{m}^{-2}\ \mathrm{s}^{-1}) = 3.4 \times 10^{-20} M^{-1.22}$ where M (kg) is the meteoroid mass (and this relationship is likely to hold down to about 10^{-7} g, with value of α being accurate probably to ± 0.1). By use of the penetration formula given in Eq. 1, and integrating over each stream's mass distribution, the instantaneous flux as a function of solar longitude, for a penetration limit $F_{max} = 1$ mm was obtained. This is shown in Fig. 3. The upper, solid curve shows the results obtained for a detector mounted perpendicularly to all streams, and hence gives an upper level for any instantaneous exposure. The lower, dotted curve is for a detector mounted on the space face of a gravity stabilised LEO spacecraft (like the Long Duration Exposure Facility) with its orbit parallel to the ecliptic plane (hence the contribution from very northern showers is greatly reduced). The model accounts for full impact geometry and Earth shielding effects. The mean value of this curve is shown, with the annual mean level also shown for comparison, as derived for the space face detector using the Grün flux (with gravitational enhancement to LEO). It is seen that at this size regime, ~10% of the Grün flux prediction is obtained purely from the 50 streams. It is also seen that the instantaneous contributions of some 7 or 8 streams (including the Leonids) would just exceed the background, although by detector collimation the 'background' could be readily suppressed.

The results in Fig. 3 are calculated at a given penetration limit. However we can consider the relative contributions of the streams if using the various detection techniques discussed above. Fig. 4 shows the the instantaneous flux throughout the year, for meteoroids in the $F_{max} = 1$ mm size regime, but now also with the relative strengths based on detection thresholds applicable to plasma charge production, and plasma current production. Note the importance of the Leonid stream (shown here without any storm enhancement) which exceeds all others in the 'plasma regime'. In the event of a Leonid storm, the peak flux could increase by orders of magnitude. To calculate the maximum meteoroid mass intercepted we can 'invert' the Grün flux distribution. This is shown in Fig. 5a. We can also consider the maximum penetration in aluminium to a real space face surface orbiting in LEO or GEO, as a function of the area-time product a_t (m^2 s); shown in Fig. 5b. Functions are fitted to the curves in Fig. 5 over the range shown, for the LEO surfaces:

$$F_{max}(\mu m) = [(1340 a_t)^{-0.126} + (2.02 \times 10^{-4} a_t)^{-0.620}]^{-2.193} \quad (7)$$

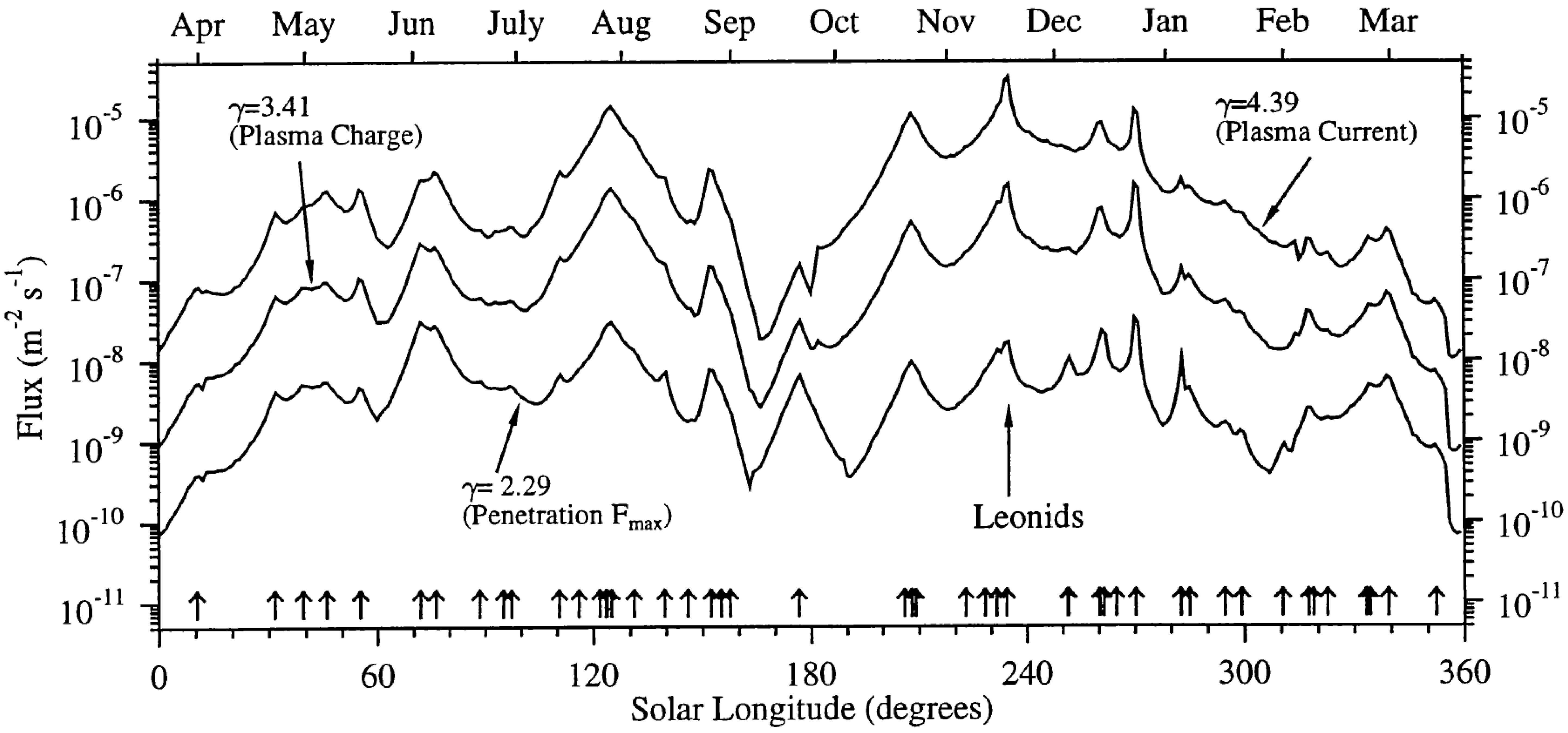

Figure 4: The instantaneous flux throughout the year, for meteoroids in the $F_{max} = 1$ mm size regime, but now also with the relative strengths based on detection thresholds based on plasma charge production, and plasma current production. Note the importance of the Leonid stream (shown here without any storm enhancement).

$$M(\mathrm{g}) = [(5.02 \times 10^{-15} a_t)^{-0.152} + (4.49 \times 10^{-8} a_t)^{-0.716}]^{-5.128} \quad (8)$$

where a_t is the area-time product (m^2 s). For GEO surfaces, the functions still apply, but instead of using a_t, we use $a_t/1.67$. Examples using this formulae, are shown in Table 3, for a typical Shuttle 2-week mission and LDEF's 5.78 year exposure.

Mission	Area-time	Mass (g)	F_{max}
Shuttle	7.3×10^8	5.4×10^{-5}	~2 mm
LDEF	2.7×10^{10}	9.7×10^{-4}	~6 mm

Table 3: The maximum meteoroid mass, and aluminium penetration depth F_{max} for a typical Shuttle mission (2 weeks) and LDEF's 5.78 year exposure. For the Shuttle, half the total surface area was assumed (600 m^2), and for LDEF an effective exposure area of 150 m^2 was assumed.

Source	Mass (g)	F_{max}
Sporadics	4×10^{-5}	< 2 mm
Leonids 15,000 ZHR	2×10^{-4}	~ 3 mm
Leonids 150,000 ZHR	4×10^{-3}	~ 9 mm

Table 4: Exposure of 1 day including the Leonid storm; the maximum penetration for a suite of satellites offering 5000 m^2 exposed area. The 15,000 ZHR is equivalent to ~ 10 days of sporadic flux, whereas the 150,000 ZHR is equivalent to ~ 350 days.

For the Leonid stream, we can note the similarity between the stream mass distribution index and the Grün flux at the larger sizes, and hence deduce a similar formula to estimate the maximum penetration limit for a given exposed area, *exposed for the 1 day* incorporating the Leonid storm. If the peak ZHR reaches 15,000 then the function becomes:

$$F_{max}(\mu m) = [(1.35 \times 10^4 a_t)^{-0.126} + (2.04 \times 10^{-3} a_t)^{-0.620}]^{-2.193} \quad (9)$$

Whereas if the peak ZHR reached 150,000 then the formula is

$$F_{max}(\mu m) = [(4.66 \times 10^5 a_t)^{-0.126} + (7.03 \times 10^{-2} a_t)^{-0.620}]^{-2.193} \quad (10)$$

In this period of 1 day at that time, exposure to the sporadics would yield considerably smaller penetration and plasma effects. Table 4 shows maximum penetration for predicted Leonid peak ZHR rates of 15,000 and 150,000 respectively, as well as the sporadic prediction. The area-time product used corresponds to 5000 m^2 over 1 day, and could apply to some 1,000 satellites of 5 m^2 area — perhaps not atypical of the active suite in operation currently. The potential effect of the shower is readily observed. Less obvious is the enhancement of plasma signals displayed in Fig. 4 (shown without the storm enhancement). With a flux enhancement of even 500 (for ZHR 15,000) the peak rate of plasma current

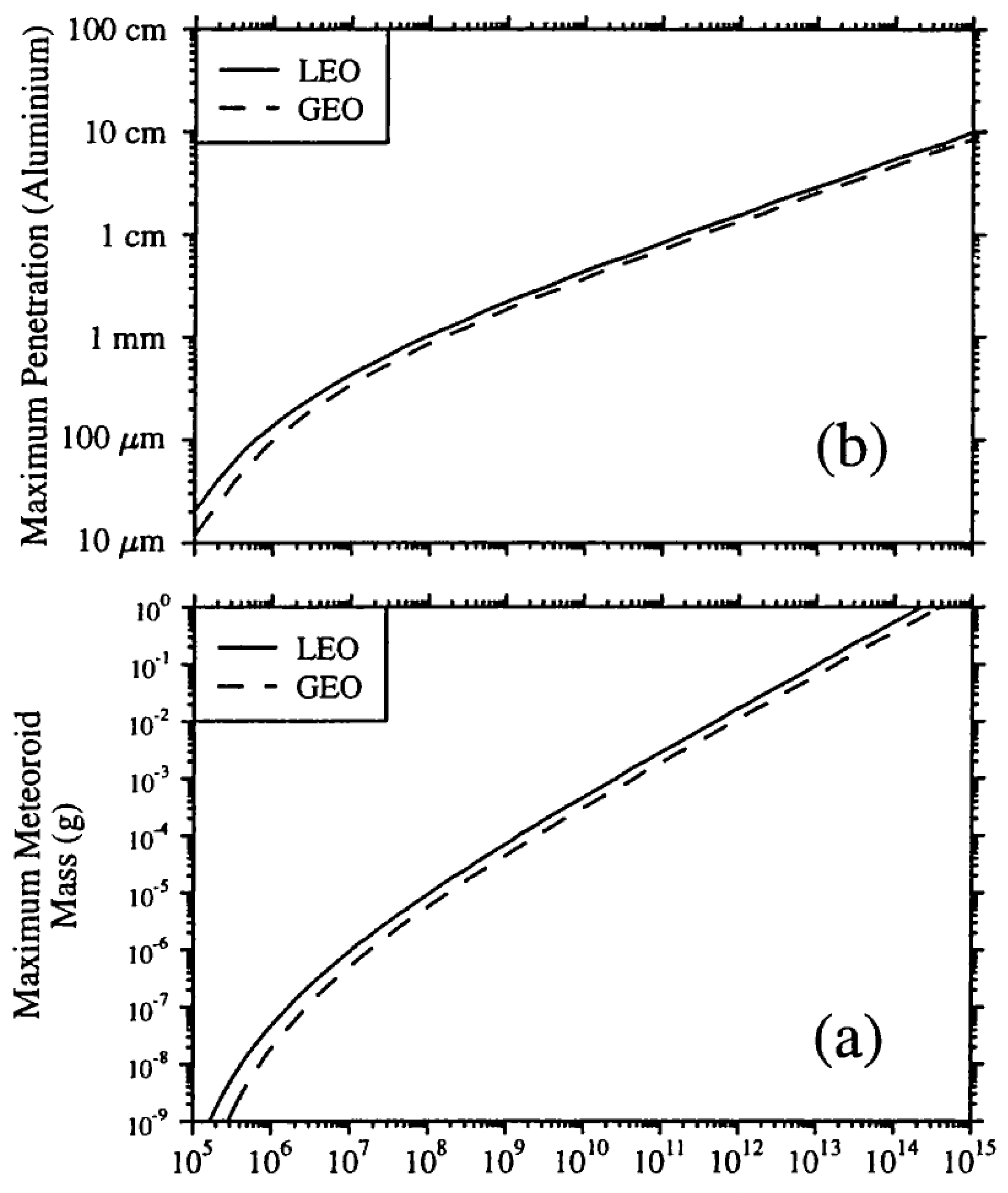

Figure 5: (a) The largest meteoroid mass encountered, and (b) the maximum aluminium penetration limit, for space pointing detectors, as a function of the exposed area-time product.

events will exceed any other stream in the year by a factor of > 1000, and the larger meteoroids impacting a spacecraft could produce a plasma current of several hundred amps if the full charge separating fields were applied by appropriate conductors.

6. CONCLUSIONS

A consideration of meteoroid flux and subsequence spacecraft effects has highlighted the significance of the Leonid stream. In storm conditions, potentially occurring in the next few years, the peak rate could well increase by a factor of 1000, and clearly dominate over the sporadic background even when integrated over a period of some days. Combined with the susceptibility of spacecraft to both penetration and to plasma effects it is appropriate to extend the modelling to predict better the likely effects and identify mitigation procedures.

7. REFERENCES

Beech, M. & Brown, P., Space platform impact probabilities — The threat from the Leonids. *ESA J.*, **18**, 63–73, 1994.

Beech, M., Brown, P. & Jones, J., The potential danger to space platforms from meteor storm activity, *Q. J. R. Astr. Soc.*, **36**, 127–152, 1995.

Beech, M., Brown, P., Jones, J., & Webster, Space platform impact probabilities during meteor storms: Leonids case study, *Planet. Space Sci.*, in press, 1997.

Caswell, R.D., McBride, N. & Taylor, A.D., Olympus end of life anomaly — a Perseid meteoroid impact event?, *Int. J. Impact Engng.*, **17**, 139-150, 1995.

Dietzel, H., Eichhorn, G., Fechtig, H., Grün, E., Hoffmann, H.-J. & Kissel, J., *J. Phys. E. Scientif. Instr.*, **6**, 209, 1973.

Gardner, D.J., McDonnell, J.A.M., Collier, I, *Int. J. Impact Engng.*, in press, 1997.

Grün, E., Zook, H.A., Fechtig, H. & Giese, R.H., Collisional balance of the meteoritic complex, *Icarus*, **62**, 244-272, 1985.

Jenniskens, P., Meteor stream activity I. The annual streams, *Astron. Astrophys.*, **287**, 990–1013, 1994.

Jenniskens, P., Meteor stream activity II. Meteor outbursts, *Astron. Astrophys.*, **295**, 206–235, 1995.

McBride, N., McDonnell, J.A.M., Gardner, D.J., Griffiths, A.D., Meteoroids at 1 AU: modelling the dynamics and properties, ESA SP-392, pp. 335–342, 1996.

McBride, N., The importance of the annual meteoroid streams to spacecraft and their detectors, *Adv. in Space Res.*, in press, 1997.

McDonnell, J.A.M., *et al.*, *Adv. Space Res.*, **4**, 297–301, 1984.

McDonnell, J.A.M., Sullivan, K., Hypervelocity impacts on space detectors: decoding the projectile parameters, in: *Hypervelocity Impacts in Space*, ed. J.A.M. McDonnell, University of Kent, pp. 39–47, 1992.

McDonnell, J.A.M., McBride, N., Ratcliff, P.R., Gardner, D.J., Griffiths, A.D. & Green, S.F., Near Earth Environment, in: *Interplanetary Dust*, University of Arizona press, submitted, 1997.

Sekanina, Z. & Southworth, R.B., Physical and dynamical studies of meteors: meteor fragmentation and stream distribution studies, NASA contractor report CR 2615, Smithsonian Institution, Cambridge, MA, 1975.

Southworth, R.B. & Sekanina, Z., Physical and dynamical studies of meteors, NASA contractor report CR 2316, Smithsonian Institution, Cambridge, MA, 1973.

Taylor, A.D., 1995a. The Harvard Radio Meteor Project meteor velocity distribution reappraised, *Icarus*, **116**, 154–158, 1995a.

Taylor, A.D., Earth encounter velocities for interplanetary meteoroids, *Adv. Space Res.*, **17**, 205–209, 1995b.

Chapter 5

Hypervelocity Impacts and Fragmentation